# Design, synthesis and evaluation of side-chain hydroxylated derivatives of lithocholic acid as potent agonists of the vitamin D receptor (VDR)

Carmen M González, Sunil Gaikwad, Gonzalo Lasanta, Julian Loureiro, Niclas Nilsson, Carole Peluso-Iltis, Natacha Rochel, Antonio Mouriño

# Design, Synthesis, Biological Activity, and Structural Analysis of Novel Des-C-Ring and Aromatic-D-Ring Analogues of 1α,25-Dihydroxyvitamin D3

Samuel Seoane, Pranjal Gogoi, Araceli Zárate-Ruíz, Carole Peluso-Iltis, Stefan Peters, Thierry Guiberteau, Miguel A. Maestro, Román Pérez-Fernández,* Natacha Rochel,* and Antonio Mouriño*

ABSTRACT: The toxic calcemic effects of the natural hormone 1α,25-dihydroxyvitamin D3 (1,25D3, 1,25-dihydroxycholecalciferol) in the treatment of hyperproliferative diseases demand the development of highly active and noncalcemic vitamin D analogues. We report the development of two highly active and noncalcemic analogues of 1,25D3 that lack the C-ring and possess an m-phenylene ring that replaces the natural D-ring. The new analogues (**3a**, **3b**) are characterized by an additional six-carbon hydroxylated side chain attached either to the aromatic nucleus or to the triene system. Both compounds were synthesized by the Pd-catalyzed tandem cyclization/cross coupling approach starting from alkyne **6** and diphenol **8**. Key steps include a stereoselective Cu-assisted addition of a Grignard reagent to an aromatic alkyne and a Takai olefination of an aromatic aldehyde. The new compounds are noncalcemic and show transcriptional and antiproliferative activities similar to 1,25D3. Structural analysis revealed that they induce a large conformational rearrangement of the vitamin D receptor around helix 6.

## INTRODUCTION

For historical reasons, the secosteroid **1a** (Figure 1) is still called vitamin D3, but it is not a true vitamin because it is produced in humans by exposure of 7-dehydrocholesterol to sunlight in the skin.[1−4] Vitamin D3 undergoes two consecutive hydroxylations to be transformed into its biologically active form 1α,25-dihydroxyvitamin D3 (**1b**, calcitriol, 1,25D3), which behaves like the classical steroid hormones such as testosterone, estradiol, and progesterone.[5] The hormone 1,25D3 binds in the kidney and other organs and tissues to the vitamin D receptor (VDR), which belongs to the superfamily of nuclear receptors. The ligand−VDR complex then interacts with the retinoid X receptor to form a heterodimer, which binds, with the assistance of cofactors, to specific regions of the DNA to induce the formation of proteins, which are responsible for a wide range of biological functions including the regulation of mineral homeostasis, cell differentiation-proliferation, apoptosis, and the immune system.[6−8] Despite the wide range of biological activities, the clinical applications of the hormone 1,25D3 have been limited due to its collateral hypercalcemic effects.[9] This problem has sparked interest in the development of less hypercalcemic and more selective 1,25D3 analogues for the treatment of hyperproliferative diseases, and a few synthetic noncalcemic analogues are already being successfully used in the treatment of psoriasis. Most of the 1,25D3 analogues developed to date are modified in the side chain and A-ring, but only a few having structural alterations in the C-ring and/or D-ring have been developed due to synthetic difficulties. Biological studies on 1,25D3 analogues that lack the D-ring, C-ring, the bicyclic CD-ring, or are modified on the C- or D-rings show that the native CD-core is not mandatory for biological activity and its alteration can reduce the calcemic activity.

A decade ago, we started a program aimed at the synthesis of vitamin D analogues having an aromatic D-ring such as (Figure 1), where the natural five-membered D-ring is replaced by a benzene nucleus.[49] Both the Pd(0)-catalyzed cyclization/Suzuki−Miyaura cross-coupling approach[50] and the dienyne approach[51] allowed access to this type of compounds. However, the vitamin D triene system of 2a unexpectedly equilibrated to a large extent at room temperature to the previtamin D form 2b via [1,7]-H sigmatropic shift.[49,52,53] This drawback led us to explore the synthesis of a series of 1,25D3 analogues

that lack the C-ring and possess an aromatic D-ring. PG-136 (Figure 1) is an example of this new class of highly active and noncalcemic 1,25D3 analogues.[54]

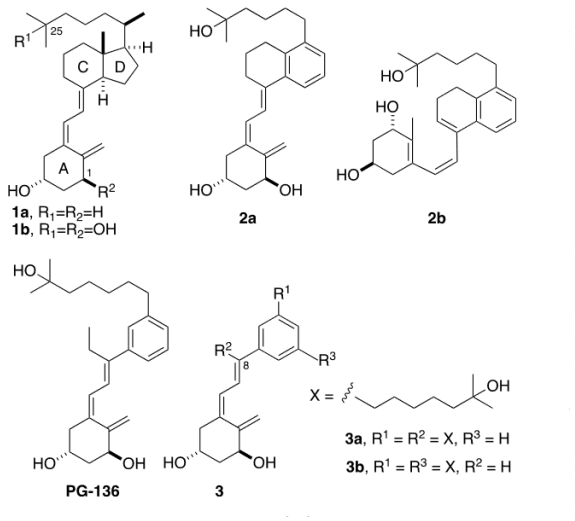


Figure 1. Structures of vitamin D3 (**1a**), 1,25-dihydroxyvitamin D3 (**1b**, 1,25D3, calcitriol), aromatic D-ring analogue **2** in the vitamin D form (**2a**) and previtamin D form (**2b**), des-C-ring and aromatic-D-ring analogue PG-136, and target des-C-ring and aromatic-D-ring analogues **3a** and **3b**.

To demonstrate the structural versatility and flexibility offered by this class of des-C-ring and aromatic D-ring 1,25D3 analogues for the construction of new analogues of therapeutic potential, we describe here the design and synthesis of the new potent and noncalcemic analogues **3a** and **3b**, which have an additional hydroxylated side chain attached to the triene system and aromatic nucleus, respectively. Analogues of 1,25D3 with two hydroxylated side chains attached to different parts of the vitamin skeleton are also known.[12,36,55]

## RESULTS AND DISCUSSION

**Docking Studies**. To gain an idea of a possible binding pose, docking studies were carried out using the GOLD program[56] with the human hVDR LBD-1,25D3 crystal structure (PDB 1DB1)[57] that corresponds to a truncated construct, which lacks the flexible insertion domain in the ligand-binding domain (LBD) and that has been successfully crystallized in complex with several 1,25D3 analogues.[58] The docking studies employing the hVDR LBD have proven useful in designing active analogues of the hormone, including VDR superagonists.[58,59] The scoring of **3a** (88% of 1,25D3) is lower in comparison to **3b** (100% of 1,25D3), which might be explained by the higher steric demand of the second side chain in the rigid protein structure. In general, the A-ring of both compounds' docking poses matches the position of the natural ligand, with **3a** showing a slight offset of 1.7 Å concerning the 1-hydroxy group. The hydrogen bonding with Ser237 and Arg274 on the one hand and Ser278 on the other was preserved for both compounds. **3a** also forms hydrogen bonding with Tyr143. Additionally, both compounds form hydrogen bonds via one hydroxyl group at the tip of one side chain with the crucial His305 and His397. However, only the hydroxyl group matches the exact position of the natural ligand, while the side chain itself is located toward helices H5 and H12 for **3a** or toward helix H7 for **3b**. For both compounds, there was an interaction with Phe422 and Val418 of H12, which is crucial for transcription interaction. The distance to the residues was shorter in comparison to 1,25D3 (5.13 Å to Phe422 and 4.69 Å to Val418).

The aromatic cores of **3a** and **3b** adopt different poses than the natural ligand standing perpendicular to the position of the C- and D-ring of 1,25D3, in order to allow the side chains of 3a and 3b to extend toward the two histidines. The second side chain of both compounds was coiled in the center of the LBD, with the side chain from **3a** attached to the triene system occupying more or less the space of the C-ring and the 18-Me group, however reaching toward helix H6. The second side chain of **3b** reaches toward helix H7, forming van der Waals interactions with Trp286, Val300, and Leu313 (Figure 2). In order to gain a better understanding of a possible binding mode and to remove the constraint from the rigid docking studies, we performed molecular dynamic (MD) calculations. The simulation can give valuable insight into receptor behavior upon binding of a ligand. Lamblin et al. gave a good example for using MD to simulate the side chain movement of the human VDR after binding a ligand over time.[60] However, the generated data represent only a simulated structure compared to an experimental X-ray structure of the ligand/receptor complex. In our study, we used the YASARA suite [61,62] with the Amber14 Force Field and a simulation time of 20 ns. The main interactions with His305, His397, Ser237, and Arg274 were preserved for **3a**. Interestingly, the MD calculation led to an unfolding of the second side chain, thus reaching further toward helix H7 and the loop 6/7. The hydroxyl group formed a π−hydrogen interaction with His305. Through this extension, helix 6 is moved by 2.3 Å, therefore increasing the size of the binding pocket. Alignment of the receptor after simulation and the X-ray structure 1DB1 resulted in an rmsd = 0.885 Å (Figure 2C). For **3b**, the MD calculation did not result in an unfolding of the second side chain. In general, the binding pose and the interactions were nearly the same as in the docking pose; however, the A-ring moved by ∼2 Å in the direction of helices H7 and H11 while preserving the hydrogen bonding of the A-ring hydroxyl groups. The bis-methyl hydroxyl head group of the second side chain also moved by ∼2 Å, however without changing the general position. Alignment gave an rmsd = 1.092 Å between 1DB1 and the simulated receptor (Figure 2F).

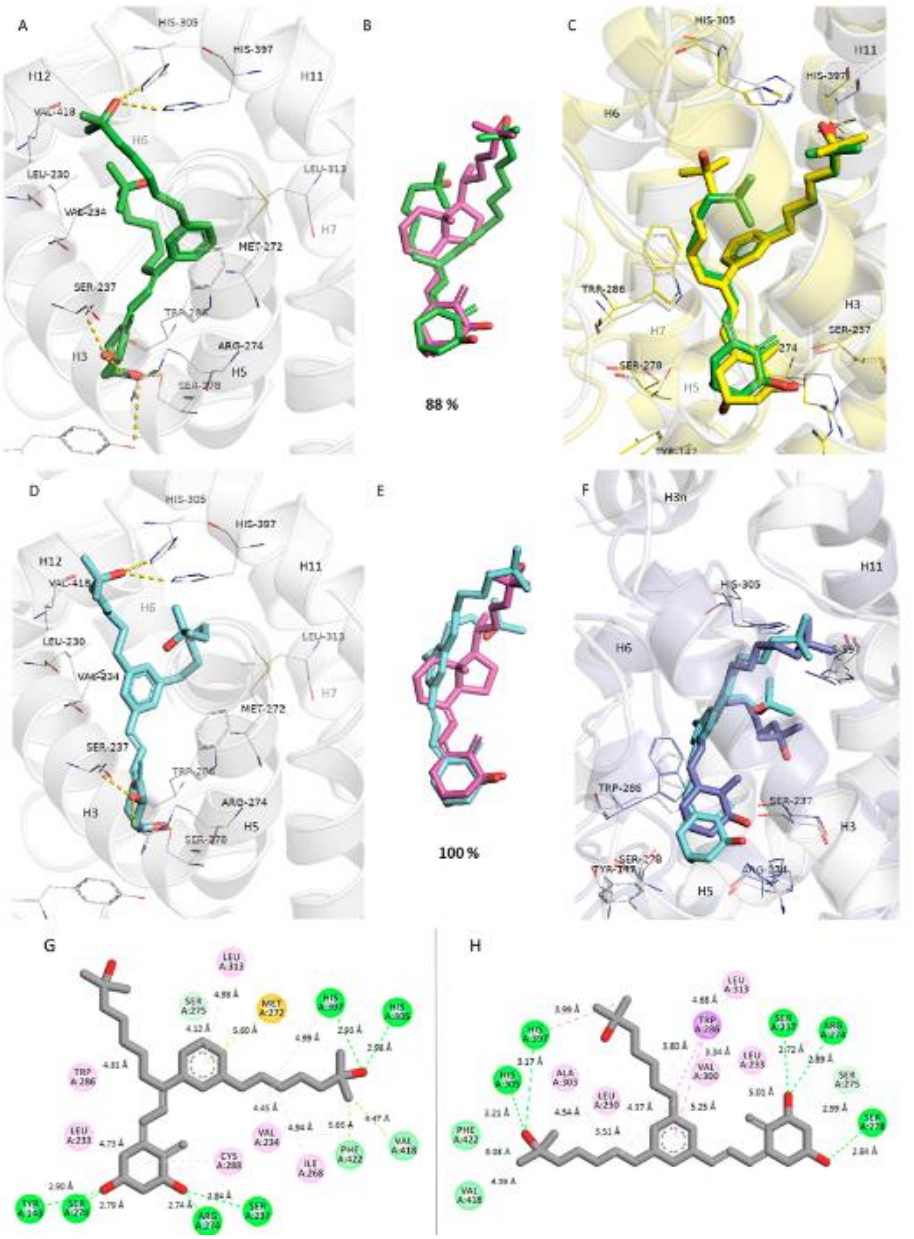


Figure 2. (**A**) Docked pose of **3a** (green) in human 1,25D3-hVDR LBD (white, PDB 1DB1). Hydrogen bonding is indicated by dotted lines. (**B**) Overlay of docking pose of **3a** with 1,25D3 (purple) extracted from the X-ray structure. Scoring (88%) is shown relative to the scoring of reference 1,25D3 (100%). (**C**) Overlay of the docking pose of **3a** (green) in the 1DB1 X-ray structure (white) with the MD-simulated structure of **3a** in 1,25D3−hVDR (yellow). Important residues are highlighted. (**D**) Docked pose of **3b** (light blue) in the 1DB1 X-ray structure. (**E**) Overlay of docking pose of **3b** with 1,25D3. (**F**) Overlay of **3b** (light blue) in the 1DB1 X-ray (white) structure with the MD-simulated structure of **3b** in 1,25D3−hVDR (blue). (**G**) Docking interactions of **3a** with hVDR. Hydrogen bondings are highlighted in green. Lipophilic interactions are highlighted in purple. π−π interactions are highlighted in deep purple, and sulfur−π interactions are highlighted in orange. (**H**) Docking interactions of **3b** with hVDR.

**Retrosynthetic Analysis**. The synthetic plan for the target compounds **3a** and **3b** (Scheme 1) involves the use of the aqueous palladium(0)-catalyzed tandem Heck-A-ring closure on enol-triflate **5** and Suzuki−Miyaura coupling with the CD-fragments 4 and 7 for the construction of the respective vitamin D trienic systems.[50] The alkenyl boronates **4** and **7** were envisioned to arise from the corresponding iodides by palladium(0)-catalyzed iodo-boron interchange following Miyaura's modified method.[50,63] We chose alkyne 6[54] and commercially available 3,5-dihydroxybenzoic acid methyl ester (**8**) as the starting materials for the respective preparation of boronates **4** and **7**.

Scheme 1. Retrosynthetic Analysis for Target 1,25D3-Analogues **3a** and **3b**.

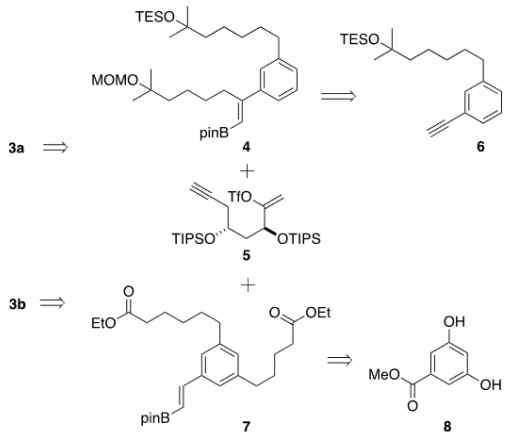


**Synthesis of Target Vitamin D Analogue 3a.** The synthesis of **3a** commenced with the known protected alkyne **6** (Scheme 2), which was prepared in 66% yield from 3-bromobenzaldehyde as previously described.[54] Cu-assisted addition of Grignard reagent **9c** to alkyne **6** in the presence of lithium chloride and subsequent trapping of the resulting Cu-alkenyl intermediate with trimethylsilyl chloride in hexamethylphosphoramide provided the trimethylsilyl intermediate **10** (89% yield), which was converted to iodide **11** by treatment with N-iodosuccinimide in dichloromethane (76% yield, 67% yield for the two steps). Iodide **11** was converted to boronate **4** in 64% yield under Miyaura's modified conditions,[50] using bis (pinacolato)diboron, potassium acetate, [1,1'-bis -(diphenylphosphino)ferrocene]dichloropalladium-(II), and tricyclohexylphosphine in dimethylsulfoxide. We then faced the formation of the triene system of 3a by Pd(0) - catalyzed ring closure of enol triflate 5 followed by cross coupling with boronate **4**. Treatment of a mixture of boronate **4** and enol-triflate **5** with a catalytic amount of bis-(triphenylphosphine)palladium(II) dichloride in aqueous potassium phosphate (2 M) in tetrahydrofuran (THF),f ollowed by desilylation with tetrabutylammonium fluoride in THF and deprotection of the methoxymethyl group with cation exchange resin AG50W-X4 in methanol, furnished the desired vitamin D analogue **3a** (53% yield, 3 steps; 23% overall yield from alkyne **6**, 6 steps).

Scheme 2. Synthesis of Target 1,25D3-Analogue **3a**.

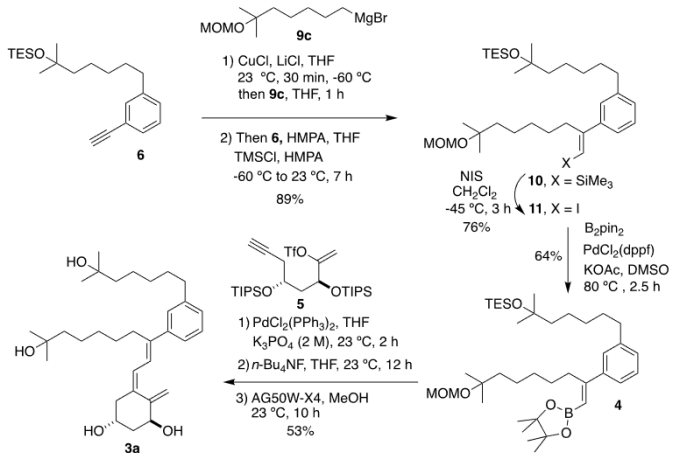


**Synthesis of Target Vitamin D Analogue 3b**. The synthesis of **3b** started with diphenol **8** (Scheme 3), which was converted in 95% yield to known ditriflate **12**[64] by treatment with triflic anhydride and triethylamine in dichloromethane. Reduction of **12** with DIBAL-H in dichloromethane provided aldehyde **13** (89% yield), which was then coupled with organozinc **14b** in the presence of catalytic palladium(II) acetate and 2-dicyclohexylphosphino-2,6-dimethoxybiphenyl in dioxane to afford diester **15** (76%), which was then converted to iodide **16** in 75% yield by treatment with chromium(II) chloride and iodoform in THF. Following the same reaction conditions as for the synthesis of **3a**, iodide **16** was converted to boronate **7** (68%), which was subjected to Pd(0)-catalyzed cyclization/cross coupling cascade in the presence of enol-triflate **5**, leading to the corresponding diester, which upon treatment with methylmagnesium bromide in THF and subsequent desilylation with tetrabutylammonium fluoride in THF afforded the desired vitamin D analogue **3b** (72% yield, 19% yield from **8**, 8 steps).

Scheme 3. Synthesis of Target 1,25D3-Analogue **3b**.

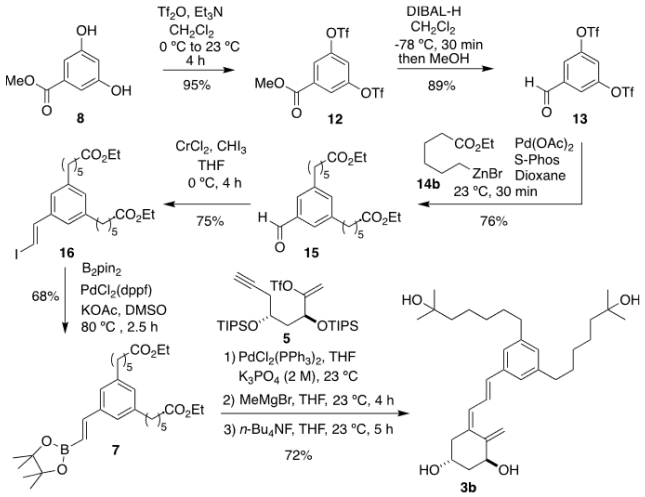


**Biological Activities and Binding**. The ligands **3a** and **3b** showed similar anti-proliferative activity to the natural 1,25D3 (**1b**) in MCF-7 cells, as shown in Figure 3A. Both **3a** and **3b** compounds significantly increase the E-cadherin protein expression, a well-known target gene of 1,25D3 (Figure 3B).65 The transcriptional activities of the CYP24A1 (24-hydroxylase) gene, another 1,25D3 target gene,[66] induced by **3a** and **3b** in MCF-7 cells are equivalent to those of 1,25D3 in the $EC_{50}$ molar range, as shown in Table 1. We next tested by competitive binding assay the biological ability of analogues **3a** and **3b** to bind VDR in comparison with the native hormone 1,25D3. VDR binding affinities of compounds **3a** and

**3b** are 20 and 10 times lower than that of 1,25D3, respectively (Table 1). Despite the high in silico binding of analogues **3a** and **3b** to the hVDR LBD in comparison with the natural hormone 1,25D3, these compounds bind weakly in vivo to the hVDR. Similar results were previously observed in structurally related des-C-ring and aromatic-D-ring analogues of 1,25D3[54] and are explained by increased interactions of the ligands, with residues of H12 allowing one to activate transcription independently of the low binding. In addition, neither **3a** nor **3b** induced hypercalcemia in mice after 21 days of treatment (Figure 3C). The remarkable lack of calcemic activity of **3a** and **3b**, together with their significant anti-proliferative and transcriptional activities in breast cancer cells, suggest their therapeutic potential in the treatment of breast tumors.[67]

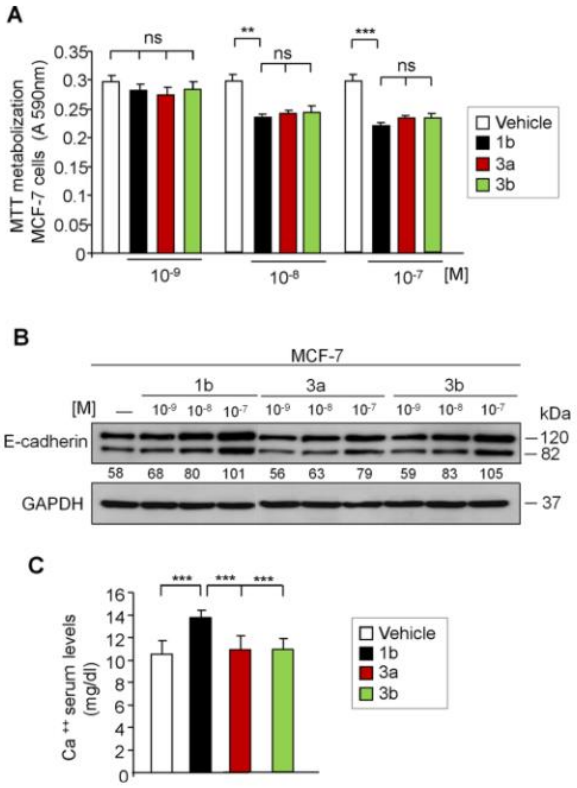


Figure 3. Biological evaluation of **3a** and **3b** in comparison with the natural hormone 1,25D3 (**1b**) (**A**) cell proliferation/cytotoxicity in human breast adenocarcinoma MCF-7 cells after treatment with **1b**, **3a**, and **3b** ($10^{-9}$ to $10^{-7}$ M) for 48 h. (**B**) Western blot of E-cadherin (a vitamin D target gene) and GAPDH (loading control) 48 h after treatment with **1b**, **3a**, and **3b** ($10^{-9}$ to $10^{-7}$ M). Quantification of E-cadherin after normalization with respect to GAPDH expression is shown. (**C**) Calcium levels in sera of mice after 21 days of treatment (0.3 μg/kg every other day) with sesame oil (as a vehicle) and **1b**, **3a**, and **3b** compounds. Results are expressed as mean ± SD. ** = $p < 0.01$; *** = $p < 0.001$; ns = not significant.

Table 1. Transcriptional Activity and VDR Binding of the Natural Hormone **1b** and Analogues **3a** and **3b**[a]

| | **Transcriptional activity** | **VDR binding** |
|---|---|---|
| | **$EC_{50}$ M range (%)** | **$IC_{50}$ M range (%)** |
| **1b** | $3.02 \times 10^{-9}$ (100%) | $1.24 \times 10^{-9}$ (100%) |
| **3a** | $5.60 \times 10^{-9}$ (54%) | $2.73 \times 10^{-8}$ (4.5%) |
| **3b** | $2.96 \times 10^{-9}$ (102%) | $1.57 \times 10^{-8}$ (7.9%) |

[a]Transcriptional activity (measured as the induction of the CYP24A1 gene luciferase-reporter vector in MCF-7 cells) is expressed as $EC_{50}$ molar (M) and as a percentage of the $EC_{50}$ M with respect to **1b**

(100%). The $EC_{50}$ values are derived from dose−response curves (from $10^{-10}$ to $10^{-6}$ M) and represent the analogue concentration capable of increasing the luciferase activity by 50%. VDR binding of **1b**, **3a**, and **3b** expressed as an $IC_{50}$ M range ($10^{-10}$ to $10^{-6}$ M) and as a percentage of the $IC_{50}$ M mean with respect to **1b**.

**Crystal Structures of VDR LBD Complexes**. The docking data were substantially corroborated by the crystal structures of **3a** and **3b** in complex with zebrafish (z) VDR LBD and a peptide encompassing the second LXXLL motif of NCoA1 solved by X-ray crystallography to a resolution of 2.6 Å. Note that we have previously shown that the binding of 1,25D3 to zVDR LBD is similar to that of hVDR LBD [68,69] and to that of full-length hVDR.[70] The detailed statistics of diffraction data collection and structural refinement are summarized in Table S1. Both VDR complexes adopt the active conformation with H12 in agonist position, forming together with helices H3 and H4 the coactivator binding site. A discrepancy between modeling and X-ray data is observed for the conformation of the aromatic ring that is identical and parallel to zTrp314 (hTrp286 in docking) in the crystallographic complexes and in the adaptation of the LBP to accommodate the second hydroxylated side chain. The A-ring and triene system of 3a and **3b** are positioned similar to those of 1,25D3 (Figure 4A−C). For **3a**, the hydroxylated alkyl side chain attached to the aromatic ring is positioned similar to the side chain of 1,25D3 (Figure 4C). The second side chain attached to C8 of **3a** is differentially positioned compared to the previously published compound **2d** with a hexyl-hydrocarbon side chain attached to C8[54] and points toward helix H6 (Figure 5A). The terminal bis-methyl hydroxyl moiety of the side chain attached to C8 requires a significant adaptation of the binding pocket to be accommodated with a backbone shift of 2 Å of H6 accompanied by rearrangements of some side chain atoms and a 20% increase of the LBP (Figure 5A). However, the C8-hydroxylated alkyl chain is more flexible than the side chain attached to the aromatic ring as revealed by the temperature factors of the corresponding atoms. In 3b, the two hydroxylated side chains attached to the aromatic ring are differentially positioned as compared to **3a**, in order to maintain the anchoring hydrogen bonds (Figure 4C,F). One the side chain lines is on the opposite side of the LBP compared to 1,25D3, while its hydroxyl group matches the position of the 25-OH group of 1,25D3 (Supporting Information Figure S1). The second side chain of **3b** is orientated toward H6, inducing a shift of 2 Å of H6 and side chain reorientation (Figure 4).

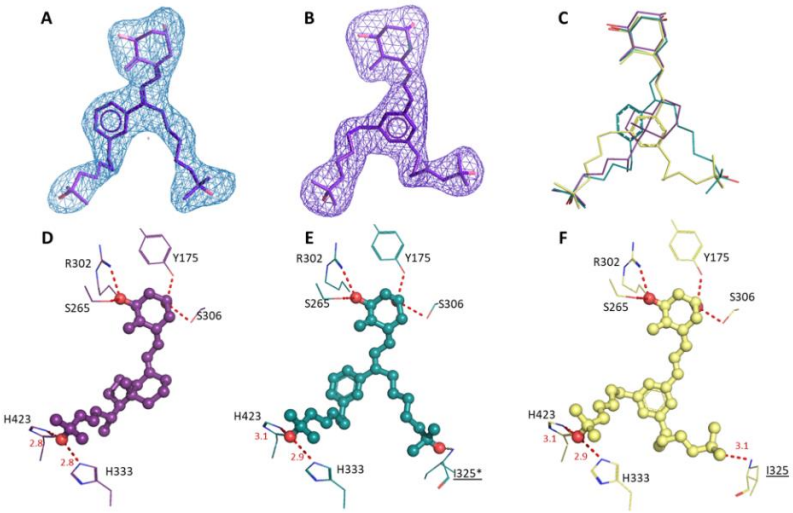

Figure 4. X-ray crystal structures of zVDR LBD complexes with **3a** (PDB 7ZFG) and **3b** (PDB 7ZFX). **3a** (**A**) and **3b** (**B**) modeled into the omit Polder maps contoured at 3σ. (**C**) Ligands **3a** (blue) and **3b** (beige) superimposed with 1,25D3 (PDB 2HC4) (purple). (**D**) Hydrogen bonds formed by 1,25D3 are shown by red dotted lines. (**E**) Hydrogen bonds formed by **3a**. *Flexible C8-hydroxylated side chain. (**F**) Hydrogen bonds formed by **3b**. Indicated distances are in angstroms.

Both compounds **3a** and **3b** form the hydrogen bonds as those formed by the hydroxyl groups of 1,25D3 (Figure 4A−C). The main differences in the interactions of the VDR−**3a** complex compared to those of the VDR−1,25D3 complex are observed for the aromatic ring that interacts more strongly with zIle299, zMet300, and zLeu341 and for the hydroxylated chain attached to C8 that interacts with residues of H6 (zCys324, zIle325, zAsp327, and zVal328) (Figure 5B). For VDR−**3b**, there are differences with VDR−1,25D3 around the two side chains attached to the aromatic ring (Figure 5D). The one that is lining the opposite pocket of the 1,25D3 side chain forms stronger interactions with zPhe448 of H12 (3.7 Å instead of 4.4 Å for 1,25D3), stabilizing the agonist conformation. The second hydroxylated chain forms additional interactions with residues of H6 (zIle325, zAsp327, and zVal328) and of H7 (zLeu338 and zLeu341). The conformational differences between **3a** and **3b** and stronger stabilization of H12 by 3b are likely the main contributions to the enhanced activity of **3b**. Other synthetic analogues such as Gemini ligands, 22-alkyl, or lactam derivatives were shown to induce structural changes in the region of loops H6−H7 or H7,[68,71−73] but none of them induced changes in H6 (Supporting Information Figure S2). In addition, in contrast to 22-alkyl or lactam derivatives that act as partial agonists or antagonists and induce side chain reorientation of rHis304 (zHis333) preventing its hydrogen bond with the hydroxyl group, analogues **3a** and **3b** maintain all hydrogen bond interactions as 1,25D3 and thus act as potent agonist ligands.

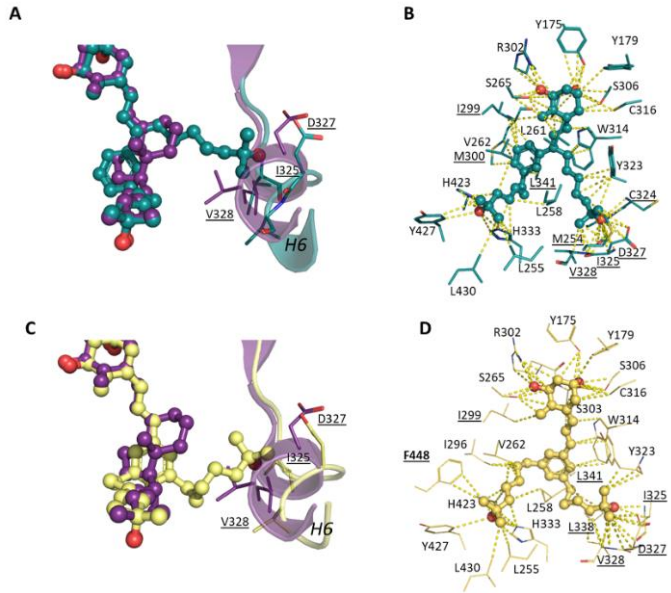


Figure 5. Interactions of **3a** and **3b** with zVDR LBD (PDB 7ZFG and 7ZFX). (**A**) Zoom around 3a-induced remodeling region of VDR (H6). Structural comparisons between zVDR LBD in complex with 1,25D3 (purple) and **3a** (blue). (**B**) Interactions of **3a** with VDR residues within a 4 Å distance. Residues interacting more strongly with **3a** compared to 1,25D3 are underlined. (**C**) Zoom around **3b**-induced remodeling region of VDR (H6). Structural comparisons between zVDR LBD in complex with 1,25D3

(purple) and **3b** (beige). (**D**) Interactions of **3b** with VDR residues within a 4 Å distance. Residues interacting more strongly with **3b** compared to 1,25D3 are underlined.

## CONCLUSIONS

Two new analogues **3a** and **3b** of the natural hormone 1,25D3, which are characterized by a des-C ring and an m-phenylene moiety that replaces the natural D-ring, were synthesized by the Pd(0)-catalyzed tandem ring-closure/Suzuki−Miyaura cross coupling approach (**3a**: 23% overall yield from alkyne **6**, 5 steps; **3b**: 19% overall yield from methyl 3,5-dihydroxybenzoate, 8 steps). Key steps in the syntheses of **3a** and **3b** include a stereoselective Cu-assisted addition of a Grignard reagent to an aromatic alkyne and a Takai olefination of an aromatic aldehyde with the CrCl2−CHI3 system, respectively. The remarkable lack of calcemic activity of **3a** and **3b**, together with their significant antiproliferative activity and transcriptional activity in breast cancer cells, suggests a therapeutic potential of these compounds for the treatment of breast tumors. Attachment of hydroxylated side chains at different positions of the aromatic D-ring opens the way for the development of new vitamin D analogues for testing.

## EXPERIMENTAL SECTION

**Docking procedure**. All structures were used as MOL2 Files. The compounds structures were generated with Chem3D. Energy minimization of the ligands was performed using the Chem3D MM2 Energy minimization tool, running the calculation to a minimum RMS gradient of 0.010 in vacuum at 300 K. Ligand structures were checked for correct stereochemistry after minimization. The crystal structure of 1,25D, obtained from the complex of 1,25DhVDR (PDB 1DB1) was used as reference ligand. Docking studies to predict the affinity of the new ligand for the VDR were carried out using the GOLD program (version Suite 5.2).[19] The protein structure was extracted from X-ray Structure 1DB1.[18] The protein was not energy minimized. A modified structure (addition of hydrogen, reconstituted gaps and corrected His tautomer His397) was used for calculations. The Ligand Binding Pocket of the reference ligand 1,25D was defined as binding site with the automatic active-site detection on, and the radius was set to 10 Å. Ligand was docked in 10 independent genetic algorithm (GA) runs, for each of which a maximum of 125000 GA operations were performed on a single population of 100 individuals. Operator weights for crossover, mutation, and migration in the entry box were used as default parameters (95, 95, and 10, respectively), as well as the hydrogen bonding (4.0 Å) and van der Waals (2.5 Å) parameters. The “flip ring corners” flag was switched off, while all the other flags were on. CHEMPLP was used as a scoring function and ChemScore as a re-scoring function. The best 3 solutions were obtained with an associated score. Docking poses were visualized with GOLD Suite and PyMOL. Structural figures were prepared using PyMOL and Discover Studio Visualizer.

**Molecular Dynamics:** The highest scoring docking pose of each ligand was taken as complex with 1,25D-hVDR (1DB1 PDB) and stored as pdb file. Molecular Dynamics calculations were performed using YASARA Suite.[28] A cubic simulation cell was created around the complex, filled with water and all charges were negated by addition of Na+ and Cl- to yield 0 net charge and a pH of 7.4. The water molecules were first annealed and a steepest energy minimization for the water molecules was performed. Excess water molecules were removed and the process was repeated. After adjusting the water molecules, 50 MD steps were performed for the waters only. Afterwards the whole system was energy minimized to remove steric constraint. Then the MD simulation started using the AMBER14 ForceField with default settings for force field terms regarding bonds, planarity, angle, van der Waals, dihedral, Coulomb and electrostatics with a 10.5 Å cutoff at a temperature of 298 K. Simulation was

run for 20 ns with a simulation substep of 1.25 fs and simulation step of 2.5 fs. Structural figures were prepared using PyMOL.

**Synthesis. Experimental procedures.**

**Preparation of ether 9b.** DMAP (0.088 g, 0.72 mmol, 0.1 equiv) and *i*-$Pr_2NEt$ (2.5 mL, 14.35 mmol, 2 equiv) were successively added to a solution of compound **9a**[29] (1.5 g, 7.17 mmol, 1 equiv) in $CH_2Cl_2$ (15 mL) at 23 ºC. The reaction mixture was cooled to 0 ˚C. After stirring for 15 min, MOMCl (1.36 mL, 17.93 mmol, 2.5 equiv) was added dropwise. The reaction mixture was stirred at 0 ˚C for 1 h and then at 23 ºC for 1.5 h. The reaction was quenched with saturated $NH_4Cl$ (20 mL) and extracted with $Et_2O$ (3 x 20 mL). The combine organic fraction was dried and concentrated. The residue was purified by flash chromatography (hexane) to afford compound **9b** [1.56 g, 6.162 mmol, 86%, $R_f$=0.5 (2% EtOAc/hexanes), colorless oil].

**Preparation of Grignard reagent 9c.** Anhydrous LiCl (1.67 g, 39.5 mmol, 2 equiv) and Mg (1.2 g, 49.37 mmol, 2.5 equiv) was dried in a reaction tube at 110 ˚C for 12 h under vacuum. Dry THF (20 mL) was added. The mixture was stirred for at 23 °C for 5 min. Mg was activated with a few drops of dibromoethane. A solution of compound **19a** (5 g, 19.75 mmol, 1 equiv) in THF (14 mL) was added *via* cannula. The mixture was vigorously stirred 23 °C for 3 h. The solution of Grignard reagent **9c** was carefully separated from the remaining Mg to another dry flask *via* a cannula.

**Preparation of (*E*)-Vinyl silane 10.** A mixture of anhydrous LiCl (0.074 g, 1.741 mmol, 2.4 equiv) and CuI (0.1724 g, 1.741 mmol, 2.4 equiv) was dried in a reaction tube under vacuum at 120 ˚C for 3 h. Dry THF (3 mL) was added. The mixture was stirred at 23 ºC for 30 min. The mixture was cooled to -60 ˚C. After 5 min, a solution of Grignard reagent **9c** in THF (7.25 mL, 4.35 mmol, 0.6M, 6 equiv) was added dropwise. The mixture was stirred at -60 ˚C for 1 h. Compound **6** (0.25 g, 0.725 mmol, 1 equiv) and HMPA (0.8 mL) in THF (5 mL) were successively added *via* cannula. A mixture of HMPA (0.4 mL) and freshly distilled TMSCl (0.23 mL, 1.814 mmol, 2.5 equiv) was added. The mixture was allowed to reach 23 ºC for 7 h and then poured into saturated $NH_4Cl$ (15 mL). The mixture was extracted with $Et_2O$ (4 x 20 mL). The combined organic fraction was dried and concentrated. The residue was purified by flash chromatography (2% EtOAc/hexanes) to afford vinyl silane **10** [0.384 g, 0.649 mmol, 89%, $R_f$= 0.33 (4% EtOAc/hexanes), colorless oil].

**Preparation of (*E*)-Vinyl iodide 11.** A solution of vinyl silane **10** (0.3 g, 0.5075 mmol, 1 equiv) in $CH_2Cl_2$ (10 mL), was cooled to -45 °C. *N*-Iodosuccinimide (0.114 g, 0.5075 mmol, 1 equiv) was added. The mixture was stirred at-45 ˚C for 3 h. The reaction was quenched with saturated $Na_2S_2O_3$ (20 mL) at -45 ˚C and allowed to reach 23 ºC. The resulting mixture was extracted with $CH_2Cl_2$ (3 x 15 mL). The combined organic fraction was dried and concentrated. The residue was purified by flash chromatography (0.5% EtOAc/hexanes) to afford vinyl iodide **11** [0.248 g, 0.385 mmol, 76%, $R_f$ = 0.3 (4% EtOAc/hexanes), light yellow oil].

**Preparation of (*E*)-alkenylboronate 4.** $PdCl_2(dppf).CH_2Cl_2$ (0.008 g, 0.0093 mmol, 0.03 equiv), KOAc (0.0912 g, 0.93 mmol, 3 equiv, dried in vacuo at 120 ˚C for 2 h) and bis(pinacolato)diboron (0.0945 g, 0.372 mmol, 1.2 equiv), were successively added to a solution of vinyl iodide **9f** (0.2 g, 0.31 mmol, 1 equiv) in DMSO (3 mL). After stirring at 80 ˚C for 2.5 h, the reaction was cooled to 23 °C. $H_2O$ was added (10 mL). The mixture was extracted with $Et_2O$ (3 x 10 mL). The combined organic fraction was dried and concentrated. The residue was purified by flash chromatography (4% EtOAc/hexanes) to afford vinyl boronic ester **4** [0.127 g, 0.197 mmol, 64%, $R_f$= 0.4 (10% EtOAc/hexanes), light brown oil].

**Preparation of vitamin D analog 3a.** Aqueous $K_3PO_4$ (2 mL, 2M) and $PdCl_2(PPh_3)_2$ (0.0054 g, 0.008 mmol, 0.05 equiv) were successively added to a solution of boronic ester **4** (0.1 g, 0.155 mmol, 1 equiv) and enol-triflate **5** (0.112 g, 0.186 mmol, 1.2 equiv) in THF (2 mL). The reaction mixture was vigorously

stirred at 23 ºC for 2 h. $H_2O$ (5 mL) was added. The mixture was extracted with $Et_2O$ (3 x 10 mL). The combined organic fraction was dried and concentrated. The residue was purified by flash chromatography (1% $Et_2O$/hexanes) to afford the protected compound which was dissolved in THF (5 mL). A solution of TBAF in THF (0.93 mL, 0.93 mmol, 1M, 6 equiv) was added. The mixture was stirred for at 23 ºC for 12 h and then diluted with saturated $NH_4Cl$ (5 mL). The mixture was extracted with EtOAc (5 x 10 mL). The combined organic fraction was dried and concentrated. The residue was purified by flash chromatography (70% EtOAc/hexanes) and the purified triol was dissolved in MeOH (10 mL). AG50W-X4 resin (3 g, freshly washed with MeOH, wet weight) was added and the heterogeneous mixture was stirred fat 23 ºC or 10 h. The mixture was filtered and successively washed with EtOAc. The solution was concentrated *in vacuo* and the residue was purified by flash chromatography (EtOAc) to afford the desired vitamin D analog **3a** [0.041 g, 0.0822 mmol, 53%, $R_f$=0.17 (EtOAc), colorless oil]. Compound **3a** was further purified by HPLC (25% *i*-PrOH/hexanes). $[\alpha]_D^{25}$= +11.7º (*c*=1.15 in EtOH).

**Preparation of 3,5-bis(trifluoromethylsulfonyloxy)benzaldehyde (13).** A solution of DIBAL-H in $CH_2Cl_2$ (3.56 mL, 3.56 mmol, 1.2 equiv, 1M) was added dropwise to a solution of compound **12** (1.4 g, 3.238 mmol, 1 equiv) in toluene (40 mL) at -78 ˚C. The reaction mixture was stirred for 30 min and then quenched with MeOH (10 mL). The mixture was allowed to reach 23 ºC for 4 h and then extracted with $Et_2O$ (3 x 30 mL). The combined organic fraction was dried and concentrated. The residue was purified by flash chromatography (8% EtOAc/hexanes) to afford aldehyde **13** [1.157 g, 2.876 mmol, 89%, $R_f$ = 0.33 (10% EtOAc/hexanes), colorless oil].

**Preparation of organozinc 14b.** Anhydrous LiCl (1.14g, 26.89 mmol, 2 equiv) was dried in a reaction tube at 160 ˚C for 20 min under high vacuum. Zn powder (1.75 g, 26.89 mmol, 2 equiv) was added under argon. The heterogeneous mixture was dried at 160 ˚C under high vacuum for 20 min. The reaction tube was evacuated and refilled with argon three times. THF (15 mL) was added and the Zn was activated with 1,2-dibromoethane (0.06 mL, 0.67 mmol, 0.05 equiv) and TMSCl (0.017 mL, 0.13 mmol, 0.01 equiv). Compound **14a** (3 g, 13.45 mmol, 1 equiv) was added and the reaction mixture was stirred at 55 ˚C overnight. The solution of **14b** was carefully separated from the remaining zinc powder with dry syringe.

**Preparation diethyl 6,6'-(5-formyl-1,3-phenylene)dihexanoate (diester 15).** $Pd(OAc)_2$ (0.0145 g, 0.065 mmol, 0.02 equiv) and S-Phos (0.053 g, 0.129 mmol, 0.04 equiv) were stirred in dioxane (3 mL) at 23 ºC for 15 min. A solution of compound **13** (1.3 g, 3.23 mmol, 1 equiv) in dioxane (7 mL) and a solution of organozinc compound **14b** in THF (13 mmol, ~4 equiv) were successively added. The reaction mixture was stirred 23 ºC for 30 min and then quenched with saturated $NH_4Cl$ (10 mL). The mixture was extracted with $Et_2O$ (20 mL x 3). The combined organic fraction was dried and concentrated. The residue was purified by flash chromatography (7% EtOAc/hexanes) to afford diester **15** [0.964 g, 2.469 mmol, 76%, $R_f$ = 0.45 (20% EtOAc/hexanes), colorless oil].

**Preparation of diethyl 6,6'-(5-(2-iodovinyl)-1,3-phenylene)(*E*)-dihexanoate (vinyl iodide 16).** Anhydrous $CrCl_2$ (0.567 g, 4.61 mmol, 6 equiv) was suspended in THF (10 mL) under argon. A solution of aldehyde **15** (0.3 g, 0.768 mmol, 1 equiv) and iodoform (0.605 g, 1.536 mmol, 2 equiv) in THF (5 mL) were successively added dropwise to the suspension at 0 ˚C. After stirring for 4 h, the mixture was poured into water (25 mL) and extracted with $Et_2O$ (3 x 15 mL). The combined organic fraction was dried and concentrated. The residue was purified by flash chromatography (7% EtOAc/hexanes) to afford vinyl iodide **16** [0.296 g, 0.575 mmol, 75% (E/Z = 14/1), $R_f$ = 0.3 (10% EtOAc/hexanes), light yellow oil].

**Preparation of diethyl 6,6'-(5-(2-(4,4,5,5-tetramethyl-1,3,2-dioxaborolan-2-yl)vinyl)-1,3-phenylene) (*E*)-dihexanoate (boronate 7).** $PdCl_2(dppf).CH_2Cl_2$ (0.012 g, 0.0146 mmol, 0.03 equiv), KOAc (0.143 g, 1.458 mmol, 3 equiv, dried in vacuo at 120 ˚C for 2h) and bis(pinacolato)diboron (0.185 g, 0.729 mmol, 1.5 equiv) were successively added to a solution of vinyl iodide **18** (0.25 g, 0.486 mmol, 1 equiv) in

DMSO (3 mL). The mixture was stirred at 80 ºC for 3 h and then cooled to 23 ºC. Water (10 mL) was added. The mixture was extracted with $Et_2O$ (3 x 10 mL). The combine organic fraction was dried and concentrated. The residue was purified by flash chromatography (5% EtOAc/hexanes) to afford vinyl boronic ester **7** [0.17 g, 0.33 mmol, 68%, $R_f$ = 0.55 (30% EtOAc/hexanes), light brown oil.

**Preparation of (1*R*,3*S*,*Z*)-5-((*E*)-3-(3,5-bis(6-hydroxy-6-methylheptyl)phenyl) allylidene)-4-methylene cyclohexane-1,3-diol (vitamin D analog 3b).** Aqueous $K_3PO_4$ (2.5 mL, 2M) and $PdCl_2(PPh_3)_2$ (0.007 g, 0.0097 mmol, 0.05 equiv) were successively added to a solution of boronic ester **7** (0.1 g, 0.194 mmol, 1 equiv) and enol-triflate **5** (0.14 g, 0.233 mmol, 1.2 equiv) in THF (3 mL). The reaction mixture was vigorously stirred at 23 ºC for 30 min. The mixture was diluted with $H_2O$ (5 mL) and extracted with $Et_2O$ (3 x 10 mL). The combined organic fraction was dried and concentrated. The residue was purified by flash chromatography (2% EtOAc/hexanes) to afford the protected compound which was dissolved in THF (5 mL). A solution of MeMgBr in THF (0.97 mL, 0.97 mmol, 1M, 5 equiv) was added at -78 ˚C. The mixture was stirred at 23 ºC for 4 h and then diluted with saturated $NH_4Cl$ (5 mL). The mixture was extracted with EtOAc (5 x 10 mL). The combined organic fraction was dried and concentrated. The residue was purified by flash chromatography (20% EtOAc/hexanes) to afford the corresponding diol, which was dissolved in THF (5 mL). A solution of TBAF in THF (0.78 mL, 0.78 mmol, 1M, 4 equiv) was added. The mixture was stirred at 23 ºC for 5 h and then diluted with saturated $NH_4Cl$ (5 mL). The mixture was extracted with EtOAc (5 x 10 mL). The combined organic fraction was dried and concentrated. The residue was purified by flash chromatography (25% *i*-PrOH/hexanes) to afford the vitamin D analog **3b** [0.07 g, 0.14 mmol, 72%, $R_f$ = 0.5 (40% *i*-PrOH/hexanes), colorless oil]. Compound **3b** was further purified by HPLC (25% *i*PrOH/hexanes). $[\alpha]_D^{25}$= +12.3º (*c*=1.46 in EtOH).

**Cell Culture.** Human breast adenocarcinoma MCF-7 cells were obtained from ATCC-LGC (Barcelona, Spain). Cells were grown in (Dulbecco's Modified Eagle Medium) DMEM media supplemented with 10% FBS, 100 U/mL penicillin, 100 U/mL streptomycin, and 2 mM L-glutamine (Sigma-Aldrich, St. Louis, USA), in air/CO2 (95:5) atmosphere a 37 °C. Cells were washed with PBS and harvested for 5 min with trypsin−EDTA solution (Sigma-Aldrich). Treatments with **1b**, **3a** and **3b** compounds were carried out using a medium without liposoluble hormones. Control cells were treated with absolute ethanol as a vehicle.

**Cell proliferation/cytotoxicity and Western blot.** Cell proliferation was carried out in MCF-7 cells using 3-(4,5-dimethylthiazol-2-yl)-2,5-diphenyltetrazolium bromide reactive (MTT) (Merck, Darmstadt, Germany). In this assay, MTT is reduced to purple formazan by the mitochondria of growing cells. Cell number increase is detected by increased MTT metabolization. Cells were plated at $1\times10^5$ cells per well in 24-well plates. Twenty-four hours later, cells were treated with 1b, 3a, and 3b ($10^{-9}$ to $10^{-7}$ M) for 48 h. Later, MTT (0.5 μg/μL) was added to each well and incubated for 1 h. DMSO (500 μL) was added to each well solubilizing cells and releasing the colorimetric reagent. The absorbance of samples was measured at 570 nm in a Mithras LB 940 from Berthold Technologies apparatus (Bad Wildbad, Germany). For Western blot, MCF-7 cells were plated ($5\times10^5$) and 24 h later treated with 1b, 3a, and 3b ($10^{-9}$ to $10^{-7}$ M) for 48 h. Expression of E-cadherin, a target gene of 1b, and GAPDH as a loading control (Santa Cruz Biotechnology, Texas, USA) were performed by Western blot as previously described.[30] E-cadherin protein expression was quantified using ImageJ software (National Institutes of Health, Maryland, USA) taking GAPDH as normalizing control.

**Luciferase Reporter Assays.** To carry out this assay, MCF-7 cells were seeded ($1\times10^5$) in 24-well plate. Twenty-four hours later cells were transfected with 1 μg of the pCYP24A1-Luc plasmid (a gift from Dr. Aranda). This plasmid code for the luciferase gene is under the control of a consensus vitamin D response element (24-hydroxylase promoter, CYP24A1). After incubation for 24 h, cells were treated with each compound (**1b**, **3a** and **3b**) at concentrations $10^{-10}$ to $10^{-6}$ M for 48 h. Luciferase was measured in Mithras LB 940 (Berthold Technologies). Dose−response curves represent the analog concentration capable of increasing the luciferase activity by 50% ($EC_{50}$ M values).

**Human VDR Binding Assay.** Binding affinity to VDR was evaluated using a 1,25D assay fluorescence polarization kit (FP)-based competition (Polarscreen Vitamin D receptor competitor assay, Invitrogen). All **1b**, **3a** and **3b** compounds were evaluated within the range from $10^{-10}$ to $10^{-6}$ M. The polarized fluorescence was measured in a 384-well black plate using a Mithras LB 940 (Berthold Technologies). The $IC_{50}$ M values were calculated using the average of measured values.

**Serum Calcium Quantitation.** Animal studies were approved by the University of Santiago de Compostela Ethics Committee for Animal Experiments. Male Swiss cd-1 mice were obtained from Santiago de Compostela University animal facilities. Mice (5 per group) were individually injected intraperitoneally either with **1b**, **3a** or **3b** (0.3 μg/kg weight) dissolved in sesame oil every other day for 21 days. Control group (n=5) was injected with sesame oil. Mice were weighed on 21 days of treatment. Calcium in serum was measured using the QuantiChom Calcium Assay Kit (BioAssay Systems, Hayward, USA).

**Biochemistry, crystallization and Structure Determination.** The cDNA encoding His-tagged zVDR LBD (156-453) was cloned into pET28b. The recombinant proteins were produced in Escherichia coli BL21 DE3 grown ON at 18 °C after induction with 1 mM IPTG at an OD600 of ~0.7. Soluble proteins were purified on Ni Hitrap FFcrude column, followed by His tag removal by thrombin cleavage and by size exclusion chromatography on HiLoad Superdex 75 column equilibrated in Tris 20mM pH7, NaCl 200mM, TCEP 1mM. The proteins were concentrated to 3-7 mg/mL with an Amicon Ultra 30 kDa MWCO. Purity and homogeneity of the proteins were assessed by SDS and Native Page. The concentrated protein was incubated with a 2-fold excess of ligand and a 3-fold excess of the coactivator NCoA1 NR2 (RHKILHRLLQEGSPS) peptide. Crystals were obtained at 293K in NaAcetate 2.5M, BisTris 0.1M pH 6.5 for VDR-**3a** and in NaActetae 2.5M, Tris 0.1M pH8 for VDR-**3b**. Protein crystals were mounted in a fiber loop and flash-cooled under a nitrogen flux after cryoprotection with 3M NaAcetate. Data collection from a single frozen crystal was performed at 100 K on the PX2 at SOLEIL (France). The raw data were processed with XDS[31] and scaled with AIMLESS[32] programs. The crystals belong to the space group $P6_522$, with one LBD complex per asymmetric unit. The structure was solved and refined using Phenix[33] and iterative model building using COOT[34]. Crystallographic refinement statistics are presented in Supplementary Table S1.

**Accession Code.** Atomic coordinates for the X-ray structure of zVDR LBD-**3a** (PDB 7ZFG) and zVDR LBD-**3b** (PDB 7ZFX) are available from the RCSB Protein Data Bank.

## AUTHOR INFORMATION


### Corresponding Authors

Román Pérez-Fernández − Department of Physiology−Center for Research in Molecular Medicine and Chronic Diseases (CIMUS), University of Santiago de Compostela, Santiago de Compostela 15706, Spain; Email: roman.perez.fernandez@usc.es

Natacha Rochel − Institut de Génétique et de Biologie Moléculaire et Cellulaire (IGBMC); Institut National de La Santé et de La Recherche Médicale (INSERM), U1258; Centre National de Recherche Scientifique (CNRS), UMR7104, Université de Strasbourg, Strasbourg, Illkirch 67400, France; orcid.org/0000-0002-3573-5889; Email: rochel@igbmc.fr

Antonio Mouriño − Department of Organic Chemistry, Research Laboratory Ignacio Ribas, University of Santiago de Compostela, Santiago de Compostela 15782, Spain; Email: antonio.mourino@usc.es

**Authors**

Samuel Seoane − Department of Physiology−Center for Research in Molecular Medicine and Chronic Diseases (CIMUS), University of Santiago de Compostela, Santiago de Compostela 15706, Spain

Pranjal Gogoi − Department of Organic Chemistry, Research Laboratory Ignacio Ribas, University of Santiago de Compostela, Santiago de Compostela 15782, Spain; Present Address: Chemical Science and Technology Division, CSIR-NEIST, Jorhat-785006, Assam, India

Araceli Zárate-Ruíz − Department of Organic Chemistry, Research Laboratory Ignacio Ribas, University of Santiago de Compostela, Santiago de Compostela 15782, Spain

Carole Peluso-Iltis − Institut de Génétique et de Biologie Moléculaire et Cellulaire (IGBMC); Institut National de La Santé et de La Recherche Médicale (INSERM), U1258; Centre National de Recherche Scientifique (CNRS), UMR7104, Université de Strasbourg, Strasbourg, Illkirch 67400, France

Stefan Peters − Department of Organic Chemistry, Research Laboratory Ignacio Ribas, University of Santiago de Compostela, Santiago de Compostela 15782, Spain; Present Address: Faculty of Applied Natural Sciences, Research Institute InnovAGe, TH Koeln, University of Applied Sciences, CHEMPARK Leverkusen, Kaiser-Wilhelm-Allee, 51368 Leverkusen, Germany.; orcid.org/0000-0002-7055-2471

Thierry Guiberteau − Laboratoire ICube-Université de Strasbourg, CNRS UMR 7357, Strasbourg 67000, France

Miguel A. Maestro − Department of Chemistry-CICA, University of A Coruñ a, A Coruñ a 15071, Spain

Complete contact information is available at:

https://pubs.acs.org/10.1021/acs.jmedchem.2c00900

**Author Contributions**

The manuscript was written through the contributions of all authors. All authors have given approval to the final version of the manuscript. S.S., P.G., A.Z.-R., C.P.I., T.G., and S.P. conducted experiments; M.A.M., R.P.F., N.R., and A.M. designed the experiments; all authors contributed to the writing of the paper.

Notes - The authors declare no competing financial interest.

ACKNOWLEDGMENTS

We thank the Xunta de Galicia (GRC/ED431B/2021/004 to AM and RP-F), FEDER/Ministerio de Ciencia, Innovación y Universidades Agencia Estatal de Investigación (PGC2018-100776-B-I00 to RP-F), and ANR-21-CE17-0009-01 (N.R.) from ANR and institutional funds from Instruct-ERIC for support and the use of resources of the French Infrastructure for Integrated Structural Biology (N.R.). We thank the German Academic Exchange Service (DAAD) for granting a fellowship. We thank CESGA for the computing time. The authors would like to thank the staff of Proxima 2 at SOLEIL for assistance in using the beamlines and Alastair McEwen (IGBMC) for help in X-ray data collections.

ABBREVIATIONS
1,25D3, 1α,25-dihydroxyvitamin D3; LBD, ligand-binding domain; VDR, vitamin D receptor

**REFERENCES**

(1) Norman, A. W. The history of the discovery of vitamin D and its daughter steroid hormone. Ann. Nutr. Metab. 2012, 61, 199−206.
(2) Wacker, M.; Holick, M. F. Sunlight and Vitamin D: A global perspective for health. Dermatoendocrinol. 2013, 5, 51−108.

(3) Deluca, H. F. History of the discovery of vitamin D and its active metabolites. BoneKEy Rep. 2014, 3, 479.
(4) Jones, G. The discovery and synthesis of the nutritional factor vitamin D. Int. J. Paleopathol. 2018, 23, 96−99.
(5) Hormones, 3rd ed.; Norman, A. W., Henry, H. L., Eds.; Academic Press, 2014.
(6) Christakos, S.; Dhawan, P.; Verstuyf, A.; Verlinden, L.; Carmeliet, G. Vitamin D: metabolism, molecular mechanism of action, and pleiotropic effects. Physiol. Rev. 2016, 96, 365−408.
(7) Bivona, G.; Agnello, L.; Bellia, C.; Iacolino, G.; Scazzone, C.; Lo Sasso, B. L.; Ciaccio, M. Non-skeletal activities of Vitamin D: from physiology to brain pathology. Medicina 2019, 55, 341.
(8) Chen, J.; Tang, Z.; Slominski, A. T.; Li, W.; Ż mijewski, M. A.; Liu, Y.; Chen, J. Vitamin D and its analogs as anticancer and anti-inflammatory agents. Eur. J. Med. Chem. 2020, 207, 112738.
(9) Jones, G.; Kaufmann, M. Update on pharmacologically-relevant vitamin D analogues. Br. J. Pharmacol. 2019, 85, 1095−1102.
(10) Maestro, M. A.; Molnár, F.; Carlberg, C. Vitamin D and its synthetic analogs. J. Med. Chem. 2019, 62, 6854−6875.
(11) Bouillon, R.; Okamura, W. H.; Norman, A. W. Structure-function relationships in the vitamin D endocrine system. Endocr. Rev. 1995, 16, 200−257.
(12) Glebocka, A.; Chiellini, G. A-ring analogs of 1,25-dihydroxyvitamin D3. Arch. Biochem. Biophys. 2012, 523, 48−57.
(13) Schmalz, H.-G.; Walzer, E. Vitamin D Active Compounds; Quinkert, G., Ed.; VCH Verlagsgesellschaft mbH: Weinheim, Germany, 1985; Vol. 3, pp 41−122
(14) Schmalz, H.-G.; Walzer, E. Vitamin D Active Compounds Part II; Quinkert, G., Ed.; VCH Verlagsgesellschaft mbH: Weinheim, Germany, 1986; Vol. 4, pp 131−258.
(15) Schmalz, H.-G.; Walzer, E. Vitamin D Active Compounds Part III; Quinkert, G., Ed.; VCH Verlagsgesellschaft mbH: Weinheim, Germany, 1987, pp 1−86.
(16) Dai, H.; Posner, G. H. Synthetic Approaches to Vitamin D. Synthesis 1994, 12, 1383−1398.
(17) Zhu, G. D.; Okamura, W. H. Synthesis of vitamin D (calciferol). Chem. Rev. 1995, 95, 1877−1952.
(18) Krause, S.; Schmalz, H.-G. Organic Synthesis Highlights; Schmalz, H.-G., Ed.; Wiley and VCH: Weinheim, Germany, 2000; pp 212−217.
(19) Chapelon, A. S.; Moraléda, D.; Rodriguez, R.; Ollivier, C.; Santelli, M. Enantioselective synthesis of steroids. Tetrahedron 2007, 63, 11511−11616.
(20) Fernandez, S.; Hernandez-Martín, A.; Gonzalez-García, T.; Ferrero, M. Synthesis of 6-s-cis and 6-s-trans A-ring modified vitamin D analogues. Curr. Top. Med. Chem. 2014, 14, 2424−2445.
(21) Fernández, S.; Ferrero, M. Strategies for the synthesis of 19-nor-vitamin D analogs. Pharmaceuticals 2020, 13, 159.
(22) Zhou, X.; Zhu, G.-D.; Van Haver, D. V.; Vandewalle, M.; De Clercq, P. J.; Verstuyf, A.; Bouillon, R. Synthesis, biological activities, and conformational analysis of four seco-D-15,19-bisnor-1α,25-dihydroxyvitamin D analogues, diastereomeric at C17 and 20. J. Med. Chem. 1999, 42, 3539−3556.
(23) Verstuyf, A.; Verlinden, L.; van Etten, E. V.; Shi, L.; Wu, Y.; D'Alleweyn, C.; Van Haver, D.; Zhu, G.-D.; Chen, Y.-J.; Zhou, X.; Haussler, M. R.; De Clercq, P.; Vandewalle, M.; Van Baelen, H.; Mathieu, C.; Bouillon, R. Biological activity of CD-ring modified 1α,25-dihydroxyvitamin D analogues: C-Ring and five-membered D-ring analogues. J. Bone Miner. Res. 2000, 15, 237−252.
(24) Eelen, G.; Verlinden, L.; Bouillon, R.; De Clercq, P.; Muñoz, A.; Verstuyf, A. CD-ring modified vitamin D3 analogs and their superagonistic action. J. Steroid Biochem. Mol. Biol. 2010, 121, 417−419.
(25) Gabriëls, S.; Van Haver, D.; Vandewalle, M.; De Clercq, P.; Verstuyf, A.; Bouillon, R. Development of analogues of 1α,25-dihydroxyvitamin D3 with biased side chain orientation: methylated des-C,D-homo analogues. Chem. Eur. J. 2001, 7, 520−532.
(26) Wu, Y.; De Clercq, P.; Vandewalle, M.; Bouillon, R.; Verstuyf, A. Vitamin D3: Synthesis of seco-C-9,11-bisnor-17-methyl-1α,25- dihydroxyvitamin D3 analogues. Bioorg. Med. Chem. Lett. 2002, 12, 1633−1636.
(27) Reddy, G. S.; Robinson, M.; Wang, G.; Palmore, G.; Gennaro, R.; Vouros, L.; De Clercq, P.; Vandewalle, P.; Young, M.; Ling, W.; Verstuyf, S.; Bouillon, A.; Bouillon, R. Removal of C-ring from the CD-ring skeleton of 1α,25-dihydroxyvitamin D3 does not alter its target tissue metabolism significantly. Arch. Biochem. Biophys. 2007, 460, 254−261.
(28) Eelen, G.; Valle, N.; Sato, Y.; Rochel, N.; Verlinden, L.; De Clercq, P.; Moras, D.; Bouillon, R.; Muñ oz, A.; Verstuyf, A. Superagonistic fluorinated vitamin D3 analogs stabilize helix 12 of the vitamin D receptor. Chem. Biol. 2008, 15, 1029−1034.
(29) Kutner, A.; Zhao, H.; Podosenin, A.; Fitak, H.; Chodynski, M.; Halkes, S. J.; Wilson, S. R. Retiferols: Design and synthesis of the new class of vitamin D analogs. In Vitamin D a pluripotent steroid hormone: Structural studies, molecular endocrinology and clinical applications; Norman, A. W., Bouillon, R., Thomaset, M., Eds.; de Gruyter & Co.: Berlin, Germany, 1994; pp 29−30.
(30) Hilpert, H.; Wirz, B. Novel versatile approach to an enantiopure 19-nor, des-CD vitamin D3 derivative. Tetrahedron 2001, 57, 681−694.

(31) Hanazawa, T.; Koyama, A.; Nakata, K.; Okamoto, S.; Sato, F. New convergent synthesis of 1α,25-dihydroxyvitamin D3 and its analogues by Suzuki−Miyaura coupling between A ring and C/D rings parts. J. Org. Chem. 2003, 68, 9767−9772.
(32) Bolla, N. R.; Marcinkowska, E.; Brown, G.; Kutner, A. Retiferols synthesis and biological activity of a conceptually novel class of vitamin D analogs. Expert Opin. Ther. Pat. 2014, 24, 633−646.
(33) Kutner, A.; Brown, G. Vitamins D: Relationship between Structure and Biological Activity. Int. J. Mol. Sci. 2018, 19, 2119.
(34) González-Avión, X. C.; Mouriñ o, A.; Rochel, N.; Moras, D. Novel 1α,25-dihydroxyvitamin D3 analogues with the side chain at C12. J. Med. Chem. 2006, 49, 1509−1516.
(35) Carballa, D. M.; Seoane, S.; Zacconi, F.; Pérez, X.; Rumbo, A.; Alvarez-Díaz, S.; Larriba, M. J.; Pérez-Fernández, R.; Muñ oz, A.; Maestro, M.; Mouriñ o, A.; Torneiro, M. Synthesis and biological evaluation of 1α,25-dihydroxyvitamin D3 analogues with long side chain at C12 and short C17 side chains. J. Med. Chem. 2012, 55, 8642−8656.
(36) Carballa, D. M.; Rumbo, A.; Torneiro, M.; Maestro, M.; Mouriñ o, A. Synthesis of 1α,25-dihydroxyvitamin D3 with β-positioned seven-carbon side chain al C12. Helv. Chim. Acta 2012, 95, 1842−1850.
(37) Carballa, D. M.; Zacconi, F.; Kulesza, U.; Mouriño, A.; Torneiro, M. Synthesis of 1α,25-dihydroxyvitamin D3 analogues with α-hydroxyalkyl substituents at C12. J. Steroid Biochem. Mol. Biol. 2013, 136, 34−38.
(38) Schepens, W.; Van Haver, D. V.; Vandewalle, M.; Bouillon, R.; Verstuyf, A.; De Clercq, P. Synthesis of spiro[4.5]decane CF-ring analogues of 1α,25-dihydroxyvitamin D3. Org. Lett. 2006, 8, 4247−4250.
(39) Eelen, G.; Verlinden, L.; Laureys, J.; Marcelis, S.; De Clercq, P.; Mathieu, C.; Bouillon, R.; Verstuyf, A. Antiproliferative and calcemic actions of trans-decalin CD-ring analogs of 1,25-dihydroxyvitamin D3. Anticancer Res. 2009, 29, 3579−3584.
(40) De Buysser, F.; Verlinden, L.; Verstuyf, A.; De Clercq, P. Synthesis of 22-oxaspiro[4.5]decane CD-ring modified analogs of 1α,25-dihydroxyvitamin D3. Tetrahedron Lett. 2009, 50, 4174−4177.
(41) Shindo, K.; Kumagai, G.; Takano, M.; Sawada, D.; Saito, N.; Saito, H.; Kakuda, S.; Takagi, K.; Ochiai, E.; Horie, K.; Takimoto-Kamimura, M.; Ishizuka, S.; Takenouchi, K.; Kittaka, A. New C15-substituted active vitamin D3. Org. Lett. 2011, 13, 2852−2855.
(42) Van Gool, M.; Zhao, X. Y.; Sabbe, K.; Vandewalle, M. Synthesis of 14,20-bis-epi-1α,25-dihydroxy-19-norvitamin D and analogues. Eur. J. Org. Chem. 1999, 1999, 2241−2248.
(43) Verlinden, L.; Verstuyf, A.; Van Camp, M. V.; Marcelis, S.; Sabbe, K.; Zhao, X.-Y.; De Clercq, P.; Vandewalle, M.; Bouillon, R. Two novel 14-epi-analogues of 1,25-dihydroxyvitamin D3 inhibit the growth of human breast cancer cells in vitro and in vivo. Cancer Res. 2000, 60, 2673−2679.
(44) Wu, Y.; Zhao, Y.; Tian, H.; Clercq, P.; Vandewalle, M.; Berthier, M.; Pellegrino, G.; Maillos, P.; Pascal, J.-C. A practical synthesis of 14-epi-19-nor-1α,25-dihydroxyvitamin D3 analogues and their A-ring epimers. Eur. J. Org. Chem. 2001, 2001, 3779−3788.
(45) Eelen, G.; Verlinden, L.; Rochel, N.; Claessens, F.; De Clercq, P.; Vandewalle, M.; Tocchini-Valentini, G.; Moras, D.; Bouillon, R.; Verstuyf, A. Superagonistic action of 14-epi-analogs of 1,25-dihydroxyvitamin D explained by vitamin D receptor-coactivator interaction. Mol. Pharmacol. 2005, 67, 1566−1573.
(46) De Clercq, P.; De Buysser, F.; Minne, G.; Schepens, W.; Vrielynck, F.; Van Haver, D. V.; Vandewalle, M.; Verstuyf, A.; Bouillon, R. The development of CD-ring modified analogs of 1α,25-dihydroxyvitamin D. J. Steroid Biochem. Mol. Biol. 2007, 103, 206−212.
(47) Minne, G.; Verlinden, L.; Verstuyf, A.; De Clercq, P. Synthesis of 1α,25-dihydroxyvitamin D analogues featuring a S2-symmetric CD-ring core. Molecules 2009, 14, 894−903.
(48) Laplace, D. R.; Van Overschelde, M. V.; De Clercq, P.; Verstuyf, A.; Winne, J. M. Synthesis of 2-ethyl-19-nor-analogs of 1α,25-dihydroxyvitamin D3. Eur. J. Org. Chem. 2013, 2013, 728−735.
(49) Eduardo-Canosa, S.; Fraga, R.; Sigüeiro, R.; Marco, M.; Rochel, N.; Moras, D.; Mouriñ o, A. Design and synthesis of active vitamin D analogs. J. Steroid Biochem. Mol. Biol. 2010, 121, 7−12.
(50) Gogoi, P.; Sigü eiro, R.; Eduardo, S.; Mouriñ o, A. An expeditious route to 1α,25-dihydroxyvitamin D3 and its analogues by an aqueous tandem palladium-catalyzed A-ring closure and Suzuki coupling to the C/D unit. Chem. Eur. J. 2010, 16, 1432−1435.
(51) Castedo, L.; Mouriñ o, A.; Sarandeses, L. Palladium-catalyzed synthesis of dienynes Related to vitamin D from enol triflates. Tetrahedron Lett. 1986, 27, 1523−1526.
(52) Eduardo-Canosa, S.; Marco, M.; Sigüeiro, R.; Mouriño, A. Studies on the synthesis of vitamin D analogs with aromatic D-ring. An. Acad. Bras. Cienc. 2018, 90, 1035−1042.
(53) Szybinski, M.; Brzeminski, P.; Fabisiak, A.; Berkowska, K.; Marcinkowska, E.; Sicinski, R. Seco-B-ring steroidal dienynes with aromatic D ring: design, synthesis and biological evaluation. Int. J. Mol. Sci. 2017, 18, 2162.
(54) Gogoi, P.; Seoane, S.; Sigüeiro, R.; Guiberteau, T.; Maestro, M. A.; Pérez-Fernández, R.; Rochel, N.; Mouriño, A. Aromatic-based design of highly active and noncalcemic vitamin D receptor agonists. J. Med. Chem. 2018, 61, 4928−4937.

(55) Maehr, H.; Lee, H. J.; Perry, B.; Suh, N.; Uskokovic, M. R. Calcitriol derivatives with two different side chains at C-20. V. Potent inhibitors of mammary carcinogenesis and inducers of leukemia differentiation. J. Med. Chem. 2009, 52, 5505−5519.
(56) Jones, G.; Willett, P.; Glen, R. C. A. R.; Leach, R.; Taylor, R. Development and validation of a genetic algorithm for flexible docking. J.Mol. Biol. 1997, 267, 727−748.
(57) Rochel, N.; Wurtz, J. M.; Mitschler, A.; Klaholz, B.; Moras, D. The crystal structure of the nuclear receptor for vitamin D bound to its natural ligand. Mol. Cell 2000, 5, 173−179.
(58) Carlberg, C.; Molnár, F.; Mouriño, A. Vitamin D receptors: The impact of crystal structures. Expert Opin. Ther. Pat. 2012, 22, 417−435.
(59) Hourai, S.; Rodrigues, L. C.; Antony, P.; Reina-San-Martin, B.; Ciesielski, F.; Magnier, B.; Schoonjans, K.; Mouriño, A.; Rochel, N.; Moras, D. Structure-based design of a superagonist ligand for the nuclear receptor of vitamin D. Chem. Biol. 2008, 15, 383−392.
(60) Lamblin, M.; Spingarn, R.; Wang, T.; Burger, M. C.; Dabbas, B.; Moitessier, N.; White, J. H.; Gleason, J. L. An o-aminoanilide analogue of 1α,25-dihydroxyvitamin D3 functions as a strong vitamin D receptor antagonist. J. Med. Chem. 2010, 53, 7461−7465.
(61) Kriege, E.; Vriend, G. New ways to boost molecular dynamics simulations. Comput. Chem. 2015, 15, 996−1007.
(62) Krieger, E.; Vriend, G. J. YASARA View-molecular graphics for all devices-from smartphones to workstations. Bioinformatics 2014, 30, 2981−2982.
(63) Ishiyama, T.; Murata, T.; Miyaura, M. Palladium(0)-catalyzed cross-coupling reaction of alkoxydiboron with haloarenes: A direct procedure for arylboronic esters. J. Org. Chem. 1995, 60, 7508−7510.
(64) Barrell, M. J.; Campañ a, A. G.; von Delius, M.; Geertsema, E. M.; Leigh, D. Light-driven transport of a molecular walker in either direction along a molecular track. Angew. Chem., Int. Ed. 2011, 50, 285−290.
(65) Pálmer, H. G.; González-Sancho, J. M.; Espada, J.; Berciano, M. T.; Puig, I.; Baulida, J.; Quintanilla, M.; Cano, A.; de Herreros, A. G.; Lafarga, M.; Muñoz, A. Vitamin D3 promotes the differentiation of colon carcinoma cells by the induction of E-cadherin and the inhibition of beta-catenin signaling. J. Cell Biol. 2001, 154, 369−387.
(66) Carlberg, C.; Muñoz, A. An update on vitamin D signaling and cancer. Semin. Cancer Biol. 2022, 79, 217−230.
(67) Vanhevel, J.; Verlinden, L.; Doms, S.; Wildiers, H.; Verstuyf, A. The role of vitamin D in breast cancer risk and progression. Endocr.-Relat. Cancer 2022, 29, R33−R55.
(68) Ciesielski, F.; Rochel, N.; Moras, D. Adaptability of the vitamin D nuclear receptor to the synthetic ligand gemini: remodelling the LBP with one side chain rotation. J. Steroid Biochem. Mol. Biol. 2007, 103, 235−242.
(69) Belorusova, A. Y.; Chalhoub, S.; Rovito, D.; Rochel, N. Structural analysis of VDR complex with ZK168281 antagonist. J. Med. Chem. 2020, 63, 9457−9463
(70) Rovito, D.; Belorusova, A. Y.; Chalhoub, S.; Rerra, A. I.; Guiot, E.; Molin, A.; Linglart, A.; Rochel, N.; Laverny, G.; Metzger, D. Cytosolic sequestration of the vitamin D receptor as a therapeutic option for vitamin D-induced hypercalcemia. Nat. Commun. 2020, 11, 6249.
(71) Huet, T.; Laverny, G.; Ciesielski, F.; Molnár, F.; Ramamoorthy, T. G.; Belorusova, A. Y.; Antony, P.; Potier, N.; Metzger, D.; Moras, D.; Rochel, N. A vitamin D receptor selectively activated by gemini analogs reveals ligand dependent and independent effects. Cell Rep. 2015, 10, 516−526.
(72) Asano, L.; Waku, T.; Abe, R. N.; Kuwabara, I.; Ito, J.; Yanagisawa, K.; Nagasawa, T.; Shimizu, T. Regulation of the vitamin D receptor by vitamin D lactam derivatives. FEBS Lett. 2016, 590, 3270−3279.
(73) Anami, Y.; Itoh, T.; Egawa, D.; Yoshimoto, N.; Yamamoto, K. A mixed population of antagonist and agonist binding conformers in a single crystal explains partial agonism against vitamin D receptor: Active vitamin D analogues with 22R-alkyl group. J. Med. Chem. 2014, 57, 4351−4367.
(74) Miyoshi, N.; Matsuo, T.; Wada, M. The Chemistry of alkylstrontium halide analogues, Part 2: Barbier-type dialkylation of esthers with alkyl halides. Eur. J. Org. Chem. 2005, 2005, 4253−4255.
(75) Martínez-Ordoñ ez, A.; Seoane, S.; Avila, L.; Eiro, N.; Macía, M.; Arias, E.; Pereira, F.; García-Caballero, T.; Gómez-Lado, N.; Aguiar, P.; Vizoso, F.; Perez-Fernandez, R. POU1F1 transcription factor induces metabolic reprogramming and breast cancer progression via LDHA regulation. Oncogene 2021, 40, 2725−2740.
(76) Kabsch, W. Software XDS for image rotation, recognition and crystal symmetry assignment. Acta Crystallogr., Sect. D: Biol. Crystallogr. 2010, 66, 125−132.
(77) Evans, P. Scaling and assessment of data quality. Acta Crystallogr., Sect. D: Biol. Crystallogr. 2006, 62, 72−82.
(78) Afonine, P. V.; Grosse-Kunstleve, R. W.; Adams, P. D. CCP4 Newsletter, 2005, 42. contribution 8.
(79) Emsley, P.; Cowtan, K. Coot: model-building tools for molecular graphics. Acta Crystallogr., Sect. D: Biol. Crystallogr. 2004, 60, 2126−2132.